IOP Conf. Series: Journal of Physics: Conf. Series **844** (2017) 012008 doi:10.1088/1742-6596/844/1/012008

Fabrication of Pattern Poled Lithium Niobate Film and its Nonlinear Optical Applications

M Xu[1], M Wang[1], Z Chen[1], J Tang[1], G Shao[1], Y Ming[1], G Cui[1] and Y Lu[1]

[1]National Laboratory of Solid State Microstructures and College of Engineering and Applied Sciences, Nanjing University, Nanjing 210093, China

E-mail: cuiguoxin@nju.edu.cn

Abstract. We develop an approach to fabricate arbitrary ferroelectric domain patterns on lithium niobate film (30-50 μm thick) by applying a structured external field at room temperature. The fabricating method can be operated easily to reach 1 μm linewidth resolution. The ferroelectric domain inversion is stable and uniform. Nonlinear diffraction is generated when the fundamental wave pumps to film. Various nonlinear wavefronts are obtained such as the frequency converted optical vortex beam. A nonlinear holographic concept is proposed to explain the physical phenomena and guide the corresponding domain design. The applications in optical field manipulation and novel photonic states generation are discussed.

1. Introduction

Lithium niobate (LN), a typical optoelectronic material, has been widely used in integrated optics due to its excellent nonlinear, electro-optic and acousto-optic properties [1-4]. Recently, the ferroelectric domain engineering on LN have attracted much attention because of the demand to realize nonlinear wave mixing process, including collinear and noncollinear situations in quasi-phase-matching (QPM) manners [5-9]. While it is difficult to carry out uniform micron linewidth ferroelectric domain inversion on typical 500-μm-thick LN crystal (the coercive field is about 21 kV/mm.) at room temperature as the result of the domain growth from +c facet to -c facet. At the same time, the domain structures will deteriorate soon for submicron LN film (540 nm thick) [10].

With the development of domain engineering applications, ferroelectric domain structure with micron or sub-micron linewidth is desired [11-14]. Here we develop a method to fabricate arbitrary ferroelectric domain patterns on LN film (30-50μm thick) by applying a structured external field at room temperature [15-16]. The ferroelectric domain inversion is stable and uniform with 1 μm linewidth resolution.

Based on the pattern poled LN film, it is convenient to observe nonlinear diffraction of vortex beam following the nonlinear holographic principle [8,17]. Furthermore, we can effectively tailor nonlinear wavefronts with designed ferroelectric domain through computer-generation holograms (CGH) [18-20]. Also, suitable domain structure could be flexibly introduced into LN for spontaneous parametric down-conversion [21].

2. Fabrication of pattern poled LN film

We develop an approach to fabricate arbitrary ferroelectric domain patterns on LN film (30-50 μm thick) by applying a structured external field at room temperature. First of all, we find out the +c facet of LN

film, and fix the LN film on the glass substrate for protection. Next, the +c facet of LN film is covered with a 1-μm-thick BCI-3511 photoresist layer by spin coating to obtain the desired pattern with maskless photolithography (SF-100, Intelligent Micro Pattern Co.). We then deposit a 120 nm thick chromium(Cr) film with electron beam evaporation (ZZSX-500, Beijing Beiyi Innovation Vacuum Technology Co.) and lift off to get a pattern electrode. Finally, the ferroelectric domain can be inverted on the designed Cr electrode pattern with the setup of Fig.1 [16]. The layer of NaCl solution can realize the ohmic contact between the ITO glass substrate and the LN film. The probes get in touch with the pattern electrode and the ITO glass substrate respectively. A pulse external electric field (the electric density E is slight higher than the coercive field, the pulse period is 1Hz, and period number is 10.) is applied to carry out the ferroelectric domain inversion.

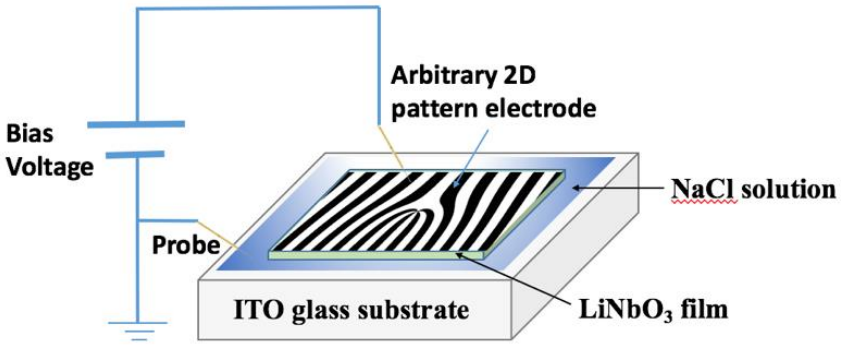

Figure 1. Setup for ferroelectric domain inversion

The most reliable technique to verify ferroelectric domain inversion is selective etching of the crystal surface. After cleaning the Cr electrode, we put the pattern poled LN film into the solution mixed by HF and H_2O_2 (1:1 in volume) at 70°C for one hour. The microscope images of LN film surfaces are recorded as shown in Fig.2 (a), (b). The minimum linewidth of each domain is about 1μm.

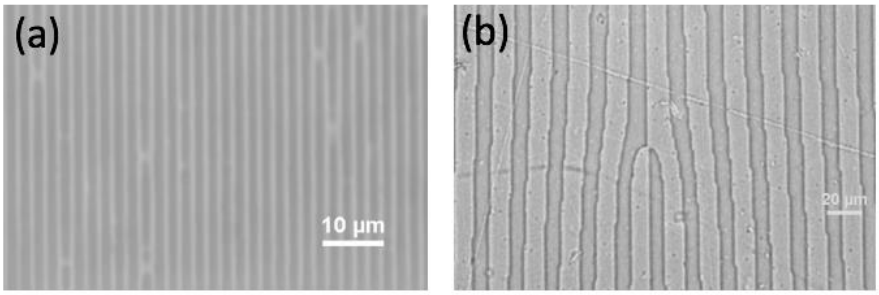

Figure 2. Microscope images of LN film surface after selective etching

There are advantages of this method to fabricate pattern poled LN film compared to typical 500-μm-thick LN crystal. This method can be operated easily and does not need extreme conditions. All the poling experiments discussed in this paper are carried out at room temperature and atmospheric pressure. At the same time, arbitrary 2D domain pattern can be generated and the ferroelectric domain inversion is stable and uniform with 1 μm linewidth resolution. The domain can consistently reach the -c facet of the film with the patterns on +c facet.

3. Nonlinear optical process of pattern poled LN film

3.1. The experimental setup

We can observe different nonlinear phenomena originated from various pattern poled LN films on a screen in the far field using the experimental setup shown in Fig.3. The fundamental pump beam from

a fs-laser (MIRA-HP & OPO, Coherent Co.), delivering 200 fs, 700 mW pulses at 1064 nm with repetition rate of 76 MHz, is directed at a small angel with respect to the Z axis. The laser beam is focused with a lens (f = 50 mm) in the plane of the pattern poled LN film. A shortpass filter is used to block the fundamental wave (FW).

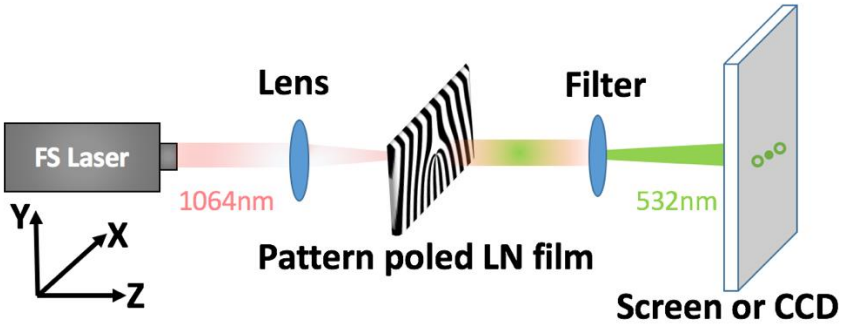

Figure 3. The experimental setup for nonlinear optical process of pattern poled LN film

3.2. Transverse QPM and nonlinear diffraction

In this paper, we will focus on second-harmonic generation (SHG), where both input beams have the same fundamental frequency (FF), $\omega_1 = \omega_2$, and the second-harmonic (SH) beam has the frequency of $\omega_3 = \omega_1 + \omega_2 = 2\omega_1$. We can use the coupled wave equation to describe the interaction between the fundamental and second-harmonic beams , which is defined in the form of: $E_i = A_i \exp[-i(k_i \cdot z - \omega_i t)], (i = 1 \; or \; 3)$, where A_i and k_i are the amplitudes and wavevectors of the fundamental wave (FW) and SH wave respectively. The equations are derived under the slowly varying amplitude approximation, and the propagation direction is set to be along the Z-axis of the LN film [22]:

$$\frac{dA_1}{dz} = \frac{2i\omega_1^2}{k_1 c^2} d_{eff} A_3 A_1^* e^{-i\Delta kz}, \quad (1)$$

$$\frac{dA_3}{dz} = \frac{i\omega_3^2}{k_3 c^2} d_{eff} A_1^2 e^{i\Delta kz}, \quad (2)$$

where d_{eff} is the nonlinear susceptibility coefficient and $\Delta k = 2k_1 - k_3$. If $\Delta k \neq 0$, the SH waves generated at different positions in the film are not in phase. This results in the destructive interference described by the factor $sinc^2(\frac{1}{2}\Delta kz)$.

We can partly satisfy the phase matching condition by modulating the sign of nonlinear coefficient along the X-axis. By inverting the ferroelectric domain orientation, the nonlinear coefficient is:

$$d(x) = d_{ij} \cdot Sign[\cos(2\pi x/\Lambda)], \quad (3)$$

where Λ is the period. And the nonlinear coefficient can also be written as an expansion of Fourier series:

$$d(x) = d_{ij} \sum_{m=-\infty}^{\infty} C_m \exp(iG_m x), \quad (4)$$

where $C_m = \frac{2}{m\pi}\sin(\frac{m\pi}{2})$ and $G_m = m\frac{2\pi}{\Lambda}$ are the mth Fourier coefficient and reciprocal vector. When the expression is substituted into Eqs. (1) and (2), we can see that the mth reciprocal vector G_m will compensates for the transverse phase mismatch as shown in Fig. 4 (c). The mth diffraction angle of nonlinear Raman-Nath diffraction is $sin(\alpha_m) = \frac{G_m}{k_2}$. And according to Snell's law, the external radiation angles are $\sin(\theta_m) = \frac{m\lambda_2}{\Lambda}$, where λ_2 is the SH wavelength. The 1st order nonlinear SH spots we measured are shown in Fig. 4 (d), which are in agreement with the theoretical calculations.

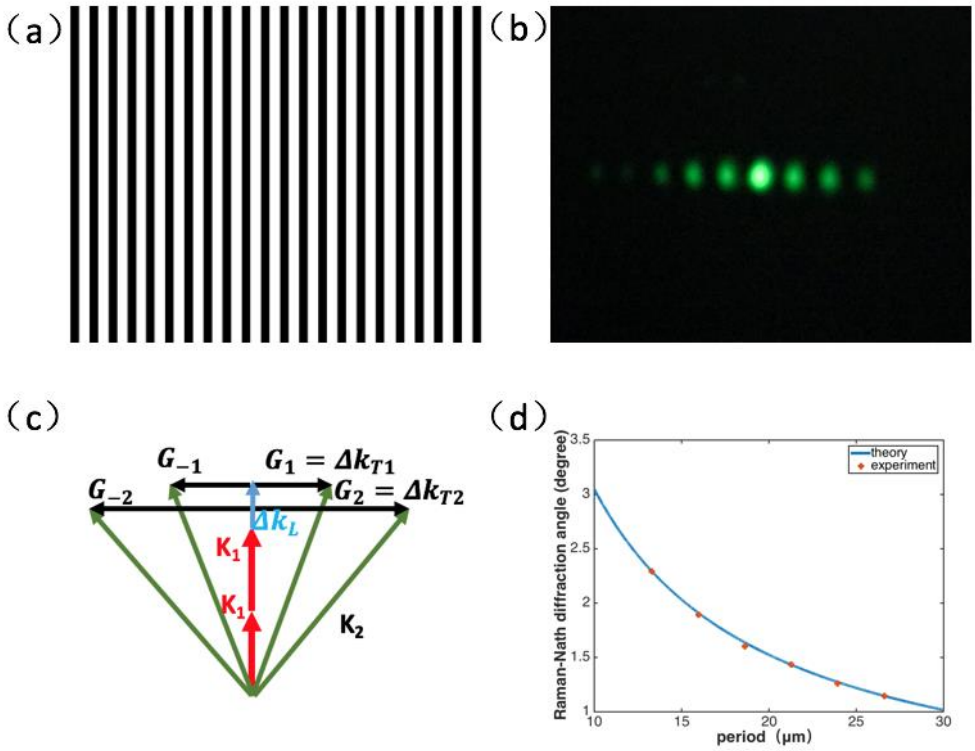

Figure 4. (a) periodic grating structure (b) nonlinear Raman-Nath diffraction (c) transverse QPM scheme (d) The 1st order nonlinear SH angels

3.3. Nonlinear holography

Holograms can be numerically computed, if the amplitude and phase of the desired wave are set as $A(x,y)$ and $\varphi(x,y)$. The amplitude transmittance of the hologram is [23]:

$$T(x,y) = 0.5\left\{1 + A(x,y)\cos\left[\frac{2\pi x}{\Lambda} - \varphi(x,y)\right]\right\}. \quad (5)$$

The desired wave is shaped in the first diffraction order as the Fourier transform of $A(x,y)\exp(i\varphi(x,y))$. We can introduce the concept of computer-generated holography (CGH) into the nonlinear optics using a binary hologram [24]:

$$T(x,y) = sign\left\{\cos\left(\frac{2\pi x}{\Lambda} + \varphi(x,y)\right) - \cos[\arcsin(A(x,y))]\right\}, \quad (6)$$

which can also be described by a Fourier series:

$$T(x,y) = \sum_{m=-\infty}^{\infty}\{\frac{\sin[m\cdot arcsin(A(x,y))]}{m\pi}\exp[im(\frac{2\pi x}{\Lambda} + \varphi(x,y))]\}. \quad (7)$$

It is obviously to see the shaped wave in the first diffraction order. So the nonlinear coefficient can be modulated to satisfy transverse QPM, and the holographic information is recorded by the ferroelectric domain inversion. We designed some patterns in our experiments. The modulation of the second-order nonlinearity coefficient of LN film is [17]:

$$d(\boldsymbol{r},\phi) = d_{ij}\cdot sign[\cos(2\pi g_{(\boldsymbol{r},\phi)})], \quad (8)$$

where $\boldsymbol{r} = x\hat{\mathbf{x}} + y\hat{\mathbf{y}}$, $\phi = tan^{-1}(y/x)$ is the azimuthal angel, d_{ij} is an element of the quadratic susceptibility tensor, $g_{(\boldsymbol{r},\phi)}$ can be arbitrary two dimensional function such as $g_{(\boldsymbol{r},\phi)} = |\boldsymbol{r}|/\Lambda$ for a concentric circles structure, or $g_{(\boldsymbol{r},\phi)} = |\boldsymbol{r}|\cos(\phi)/\Lambda + l_c\phi/2\pi$ for a fork grating structure with the topological charge (l_c), where Λ is the poling period, as shown in Fig.5 (a), (b). According to Eq. (7), we can effectively tailor nonlinear wavefronts as shown in Fig.5 (d), (e) with designed ferroelectric domains based on the nonlinear holographic method. Here $g_{(\boldsymbol{r},\phi)}$ can also be discrete lattice structure

as Fig.5 (c), and the diffraction pattern is formed by multiple QPM situations, which is recorded by CCD in Fig.5 (f).

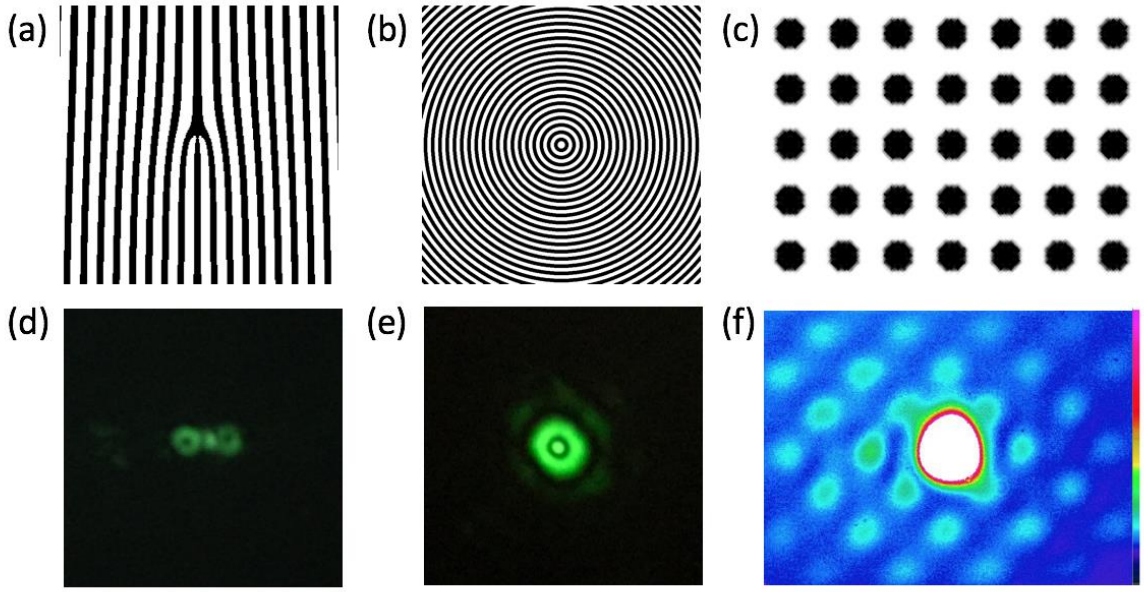

Figure 5. (a), (b) and (c) Different designs of ferroelectric domain pattern. (d), (e) and (f) corresponding nonlinear holographic patterns recorded by camera and CCD

4. Conclusion

In summary, we present a convenient method to fabricate stable arbitrary ferroelectric domain patterns on LN film at room temperature and atmospheric pressure. Nonlinear SH wave can be shaped following the nonlinear holographic principle based on pattern poled LN film, when the fundamental wave pumps to film. Various nonlinear wavefronts are obtained such as the frequency converted optical vortex beam. We can also design arbitrary domain structure in the continuous or discrete cases. Furthermore, suitable domain structures could be flexibly introduced into LN for spontaneous parametric down-conversion, which can be used in optical field manipulation and novel photonic states generation.

Acknowledgment

This work was supported by the National Natural Science Foundation of China (NSFC) (No.61490714, No. 61435008 and No. 11604144).

References

[1] Song X, Xu F and Lu Y 2011 *Opt. Lett.* **36** 4434.
[2] Shao G, Song X, Xu F and Lu Y 2012 *Opt. Express* **20** 19343.
[3] Song X,Wang Q, Yu Z, Xu F and Lu Y 2011 *J. Nonlinear Opt. Phys. Mater.* **20** 129.
[4] Hu X, Ming Y, Zhang X, Lu Y and Zhu Y 2012 *Appl. Phys. Lett.* **101** 151109.
[5] Arie A and Voloch N 2010 *Laser Photon. Rev.* **4** 355.
[6] Shapira A, Naor L and Arie A 2015 *Sci. Bull.* **60** 1403.
[7] Liu H, Li J, Zhao X, Zheng Y and Chen X 2016 *Opt. Express* **24** 15666.
[8] Fang X *et al.* 2015 *Appl. Phys. Lett.* **39** 8185.
[9] Fang X *et al.* 2016 *Opt. Lett.* **41** 1169.
[10] Shao G, Bai Y, Cui G, Li C, Qiu X, Geng D, Wu D and Lu Y 2016 *Aip Advances* **6** 075011.
[11] Sheng Y, Ma D, Ren M, Chai W, Li Z, Koynov K and Krolikowski W 2011 *Appl. Phys. Lett.* **99** 031108.
[12] Li L, Li T, Wang S, Zhang C and Zhu S 2011 *Phys. Rev. Lett.* **107** 126804.

[13] Jin H, Xu P, Luo X, Leng H, Gong Y, Yu W, Zhong M, Zhao G and Zhu S 2013 *Phys. Rev. Lett.* **111** 023603.
[14] Shapira A and Aire A 2011 *Opt. Lett.* **36** 1933.
[15] Yamada M, Nada N, Saitoh M and Watanabe K 1992 *Appl. Phys. Lett.* **62** 435.
[16] Mohageg M, Strekalov D, Savchenkov A, Matsko A, Ilchenko V and Maleki L 2005 *Opt. Express* **13** 3408.
[17] Bloch N, Shemer K, Shapira A, Shiloh R, Juwiler I and Arie A 2012 *Phys. Rev. Lett.* **108** 233902.
[18] Shapira A, Juwiler I and Arie A 2011 *Opt. Lett.* **36** 3015.
[19] Shapira A, Shiloh R, Juwiler I and Arie A 2012 *Opt. Lett*. **37** 2136.
[20] Shapira A, Juwiler I and Arie A 2013 *Laser Photon. Rev.* **7** 25.
[21] Ming Y, Tang J, Chen Z, Xu F, Zhang L and Lu Y 2015 *IEEE J. Sel. To. Quant*. **21** 6601206.
[22] Yariv A and Yeh P 1983 *Optical Waves in Crystals* (New York: John Wiley & Sons) Chap.12.
[23] Burch J 1967 *IEEE Proc.* **55** 599.
[24] Lee W 1979 *Appl. Opt.* **18** 3661.